Electronic Supplementary Material (ESI) for ChemComm.

Supporting Information

Humidity-Swing Mechanism for CO_2 Capture from Ambient Air

Hao Yang, Manmilan Singh, and Jacob Schaefer*

Department of Chemistry, Washington University, St. Louis, MO 63130, USA

*Email: jschaefer@wustl.edu (J. Schaefer)

This file includes:

14 pages

Materials and Methods

$^{13}CO_2$ absorption and desorption

To prepare the $^{13}CO_2$-absorbed sample, about 150 mg of the polymeric sorbent (Figure S1) was placed at the bottom of a three-neck round-bottom flask. The round-bottom flask was connected to a Schlenk line which in turn was connected to humidified and dry nitrogen sources. Humidified nitrogen was produced by passing dry nitrogen gas through a bubbler containing water. The round-bottom flask containing the sorbent was first evacuated by placing it under vacuum for one minute using the Schlenk line. The sorbent was then allowed to equilibrate under humidified nitrogen for one hour by passing humidified nitrogen through the round-bottom flask followed by evacuation under vacuum for one minute. Subsequently, the sorbent was equilibrated under dry nitrogen for one hour by passing dry nitrogen through the round-bottom flask, followed by lyophilization for 16 hours. Finally, the sorbent was exposed to about one liter of 90% ^{13}C-enriched CO_2 for four hours to make the final $^{13}CO_2$-absorbed sample. The $^{13}CO_2$-absorbed sample was pressed into pellets and placed in a 5-mm zirconia rotor for solid-state NMR measurements.

To prepare the desorbed sample, $^{13}CO_2$-absorbed sorbent prepared as above was placed in a three-neck round-bottom flask connected to a Schlenk line which was connected to a D_2O-humidified nitrogen source. D_2O-humidified nitrogen gas was produced by passing dry nitrogen gas through a bubbler containing 99.98% D_2O. The sorbent was allowed to equilibrate under D_2O-humidified nitrogen for 25 minutes by passing D_2O-humidified nitrogen through the round-bottom flask. The desorbed sample was pressed into pellets and placed in a 5-mm zirconia rotor for solid-state NMR measurements.

Solid-state NMR experiments

The NMR spectrometer for all the experiments except ^{13}C{^{15}N} REDOR has an 89-mm bore, 12-T static field (^{1}H at 500.5 MHz, Magnex, Agilent, Santa Clara, CA), a Tecmag (Houston, TX) Apollo console, and a homebuilt four-channel (^{1}H, ^{19}F, ^{13}C, ^{2}H) transmission-line probe equipped with a 5-mm Chemagnetics/Varian (Fort Collins, CO/Palo Alto, CA) stator and zirconia rotors. Radio-frequency pulses for ^{1}H (500.5 MHz) were amplified first by a 50-W American Microwave Technology (AMT, Anaheim, CA) power amplifier and then by a 2-kW Creative Electronics tube amplifier. AMT amplifiers (2 kW) were used for ^{13}C (125.9 MHz) and ^{2}H (76.8 MHz) pulses. For all the NMR experiments, 71 kHz pulses (7 μs for π pulses) were used for ^{1}H, ^{13}C and ^{2}H, and continuous-wave proton-decoupling strength was 71 kHz. Matched cross-polarization (CP) transfers were made at 71 kHz in 1.5 ms in ^{13}C cross-polarization magic-angle-spinning (CPMAS) echo and static ^{13}C CP echo (without spinning) experiments. Adamantane was used as an external ^{13}C chemical shift reference.[1] Spinning rates were actively controlled to 8000 ± 2 Hz. All RF pulse amplitudes were under active control (H_1 control) to eliminate long-term drifts due to component aging or changes in temperature.[2] The samples weighed between 60 and 110 mg. Each of the ^{13}C CPMAS echo experiment (Figure 1) was the result of accumulation of 40,000 scans (1 day) to 120,000 scans (3 days). For the variable-temperature static ^{13}C CP echo experiments (Figure 2 and Figure S2), each spectrum of the $^{13}CO_2$-absorbed sorbent (Figure S2a) took 120,000 scans (3 days), and each spectrum of the natural-abundance sorbent (Figure S2b) took 75,000 scans (2 days). Thus 195,000 scans (5 days) were accumulated for the measurement at each temperature, and a total of 1,365,000 scans (35 days) were accumulated for the measurements through the studied temperature range, -10, -20, -30, -40, -50, -55 and -60 °C. The ^{2}H magic-angle-spinning (MAS) Hahn echo experiment (Figure 3) was the result of accumulation of 800,000 scans (9 days) with a recycle delay of 1 sec. Each of the variable CP-contact-time ^{13}C CPMAS echo spectrum took 1024 scans. The ^{13}C MAS Hahn echo experiment took 2048 scans (3 days) with a recycle delay of 120 sec. All the experiments were acquired with a recycle delay of 2 sec except the ^{2}H and ^{13}C MAS Hahn echo experiments as mentioned above. All the experiments were measured at -10 °C except the variable-temperature ones.

The $^{13}C\{^{15}N\}$ REDOR[3-5] experiment was performed at room temperature at 12 T (^{1}H at 499.8 MHz, Magnex) with a homebuilt six-frequency transmission-line probe (^{1}H, ^{19}F, ^{31}P, ^{13}C, ^{17}O, ^{15}N) having a 12-mm long, 6-mm inner-diameter analytical coil, and a Chemagnetics/Varian ceramic spinning module. Samples were spun using a thin-wall Chemagnetics/Varian 5-mm outer-diameter zirconia rotor at 7143 Hz, with the speed under active control and maintained to within ± 2 Hz. A Tecmag Libra pulse programmer controlled the spectrometer. 2-kW AMT power amplifiers were used to produce radio-frequency pulses for ^{13}C (125.7 MHz) and ^{15}N (50.7 MHz). Radio-frequency pulses for ^{1}H (499.8 MHz) were generated by a 2-kW Creative Electronics tube amplifier driven by a 50-W AMT amplifier. All final-stage amplifiers were under active control.[2] The π-pulse lengths were 8 μs for ^{13}C and ^{1}H, 9 μs for ^{15}N. Proton-carbon-matched cross-polarization transfers were made in 4 ms at 56 kHz. Continuous-wave proton-decoupling was 100 kHz. S and S_0 alternate-scan strategy compensated for short-term drifts in REDOR experiments. Standard XY-8 phase cycling[6] was used for all refocusing π pulses (inserted at the end of each rotor period during dipolar evolution) and dephasing π pulses (inserted in the middle of each rotor period) to compensate for pulse imperfections.[7] About 100,000 scans were accumulated for each of the S and S_0 spectra (5 days) at a given dephasing time with a recycle delay of 2 sec.

Table S1: ^{13}C chemical shift anisotropy (CSA) parameters of the sorbent-absorbed CO_2 (in the form of HCO_3^- $^+N(CH_3)_3R$) and various carbonate and bicarbonate compounds.[a]

Compound		**CSA Parameters**			
		δ_{11} δ_{22} δ_{33} **/ ppm**	δ_{iso} **/ ppm**	δ_{aniso} **/ ppm**	η
carbonates	$CaCO_3$	194 194 119	169	-50	0
	$BaCO_3$	199 191 118	170	-51	0.16
	$K_2CO_3 \cdot 1.5H_2O$	204 182 122	170	-47	0.46
	$MgCO_3 \cdot 3H_2O$	204 171 120	165	-45	0.73
bicarbonates	$(NH_4)HCO_3$	223 152 119	163	58	0.57
	$KHCO_3$	218 155 113	162	56	0.75
	HCO_3^- $^+N(CH_3)_3R$[b]	225 155 110	161	62	0.73

[a] The CSA parameters (δ_{11}, δ_{22}, δ_{33} and δ_{iso}) of $CaCO_3$, $BaCO_3$, $K_2CO_3 \cdot 1.5H_2O$, $MgCO_3 \cdot 3H_2O$, $(NH_4)HCO_3$, and $KHCO_3$ are from Principal Components of Chemical Shift Tensors: A Compilation (2nd edition, ISBN 0-917903-01-3).[8]

[b] The CSA parameters (δ_{11}, δ_{22}, δ_{33}) of the sorbent-absorbed CO_2 (in the form of HCO_3^- $^+N(CH_3)_3R$) were extracted from the static ^{13}C CP echo label-only spectrum at -60 °C (Figure 2). The isotropic chemical shift (δ_{iso}) was extracted from the ^{13}C CPMAS echo spectrum (Figure 1b).

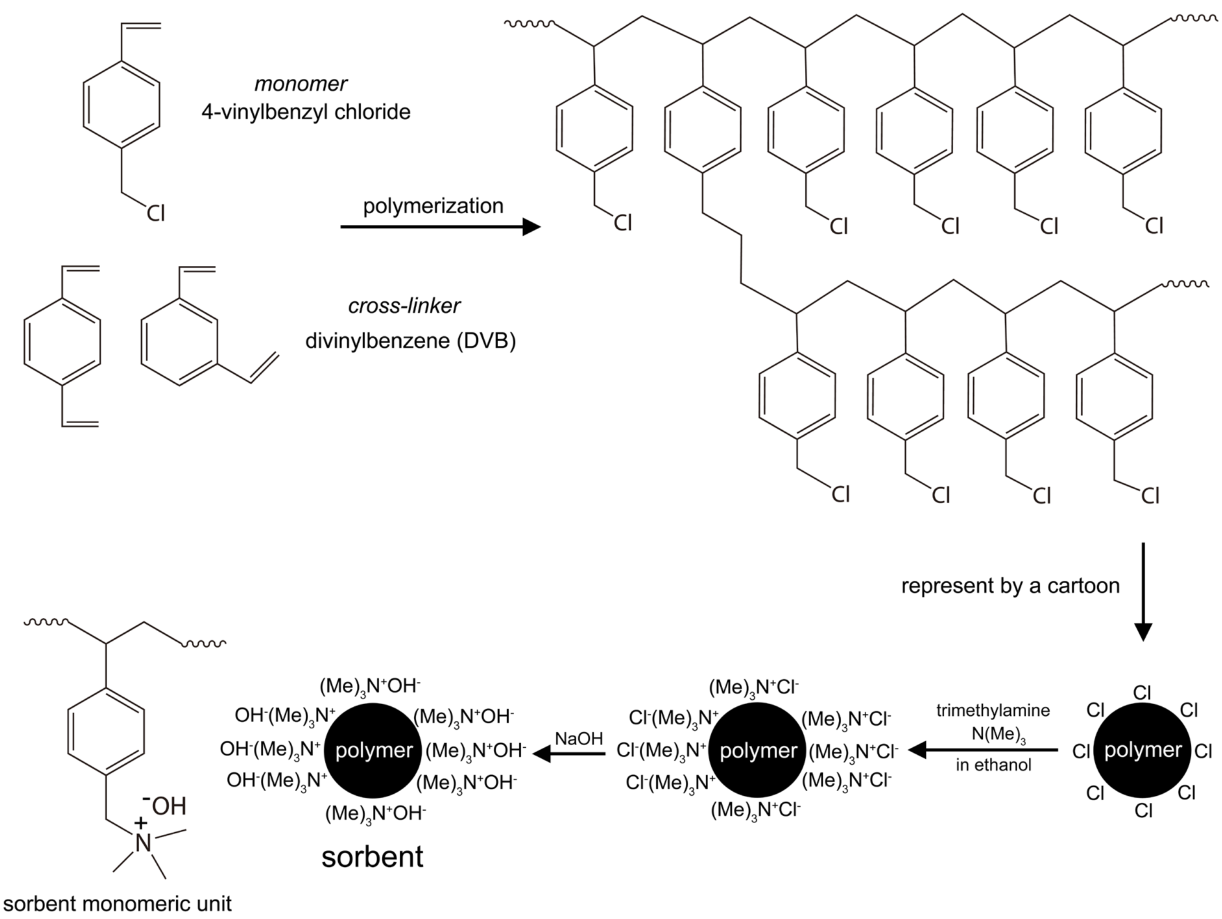

Figure S1. The synthesis scheme and chemical structure of the sorbent, which was provided by Professor Krzysztof Matyjaszewski and Professor Tomasz Kowalewski, Department of Chemistry, Carnegie Mellon University.

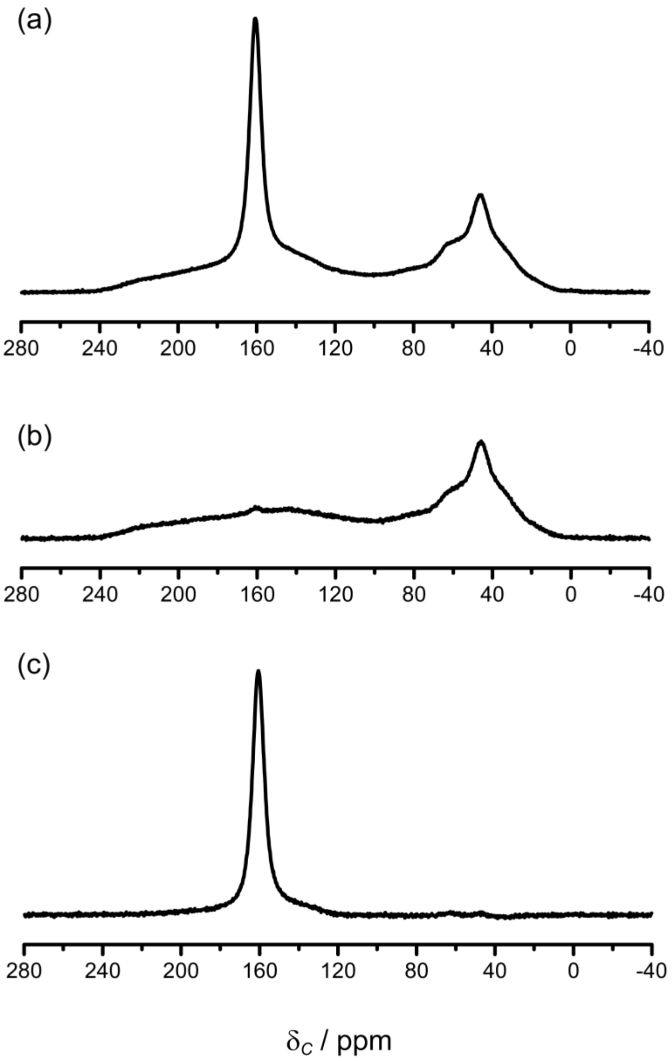

Figure S2. Static ^{13}C CP echo (without spinning) spectra at -10 °C of (a) the $^{13}CO_2$-absorbed sorbent and (b) the natural-abundance sorbent. The label-only spectrum (c) was obtained by subtracting the natural-abundance spectrum (b) from the $^{13}CO_2$-absorbed spectrum (a). The label-only spectra at -30, -50, and -60 °C were obtained in the same way (Figure 2).

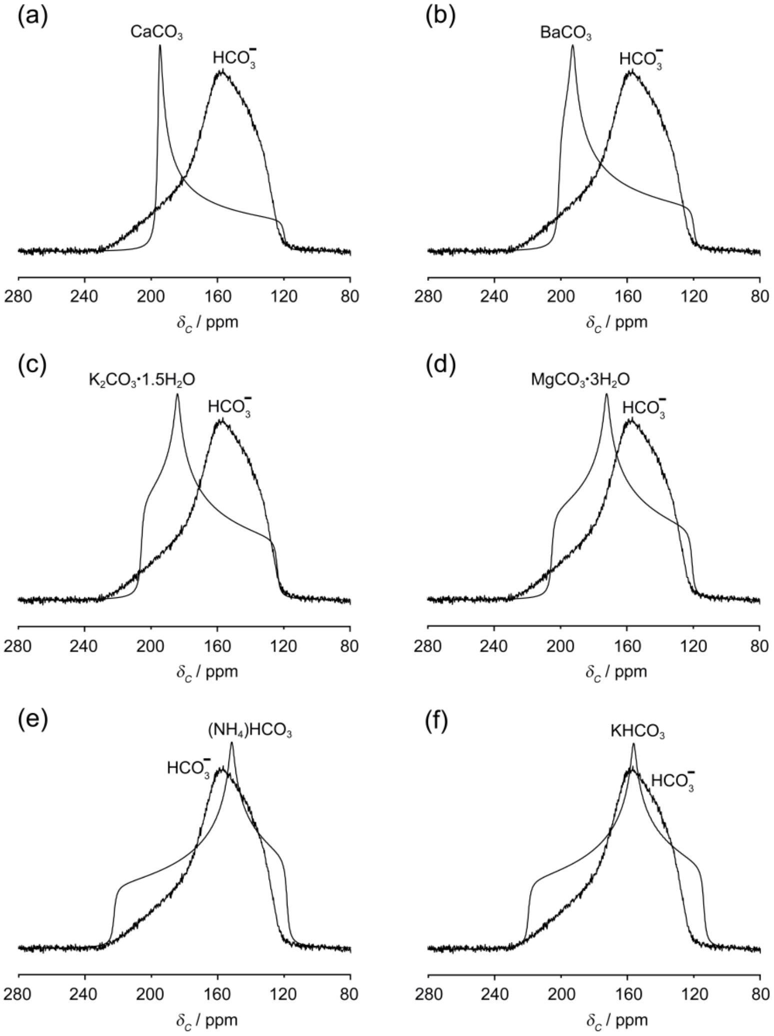

Figure S3. Comparisons of chemical-shift-anisotropy patterns of the sorbent-absorbed $^{13}CO_2$ obtained at -60 °C (Figure 2) with that of various carbonate and bicarbonate compounds: (a) $CaCO_3$, (b) $BaCO_3$, (c) $K_2CO_3 \cdot 1.5H_2O$, (d) $MgCO_3 \cdot 3H_2O$, (e) $(NH_4)HCO_3$, and (f) $KHCO_3$. The carbonates all show a negative anisotropy, where δ_{22} is closer to δ_{11} than δ_{33}[9] (also see Table S1). In contrast, the bicarbonates all show a positive anisotropy, where δ_{22} is closer to δ_{33} than δ_{11}[9] (also see Table S1). The sorbent-absorbed $^{13}CO_2$ has a positive anisotropy and a CSA pattern similar to those of bicarbonates and distinct from those of carbonates. Thus the above comparisons support the claim that the absorbed CO_2 is in the form of HCO_3^-, not CO_3^{2-}. The chemical shift patterns of the above carbonate and bicarbonate compounds were generated by simulations in SIMPSON[10] with the CSA parameters extracted from Principal Components of Chemical Shift Tensors: A Compilation (2nd edition).[8]

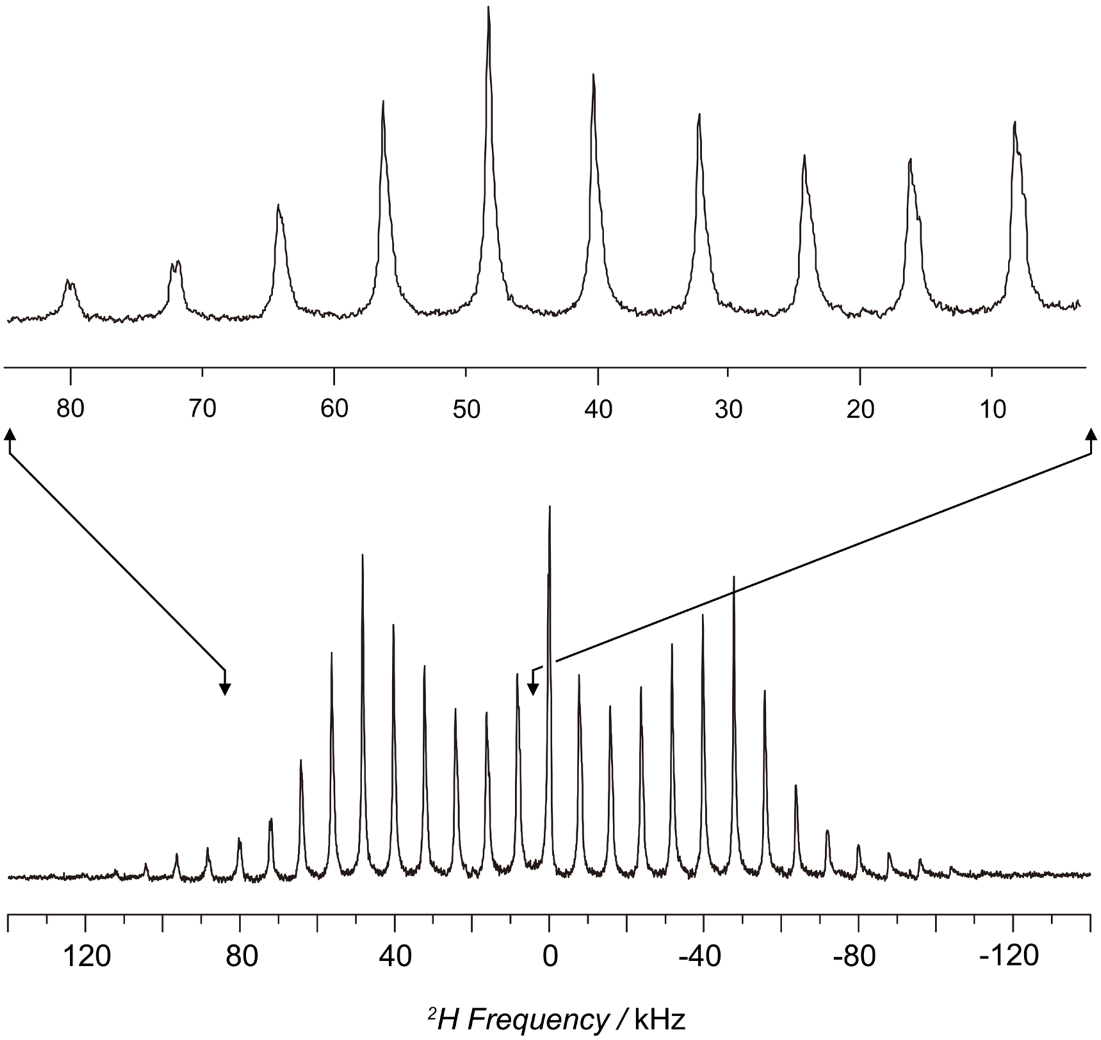

Figure S4. ^{2}H MAS Hahn echo spectrum acquired at -10 °C of the sorbent after desorbing CO_2 by bubbling D_2O-humidified N_2 gas through the $^{13}CO_2$-absorbed sorbent for 25 minutes. The top inset, zooming in on the sidebands, shows multiple chemical shifts, consistent with D_2O in a distribution of sites created by heterogeneity in the local polymer chain packing.

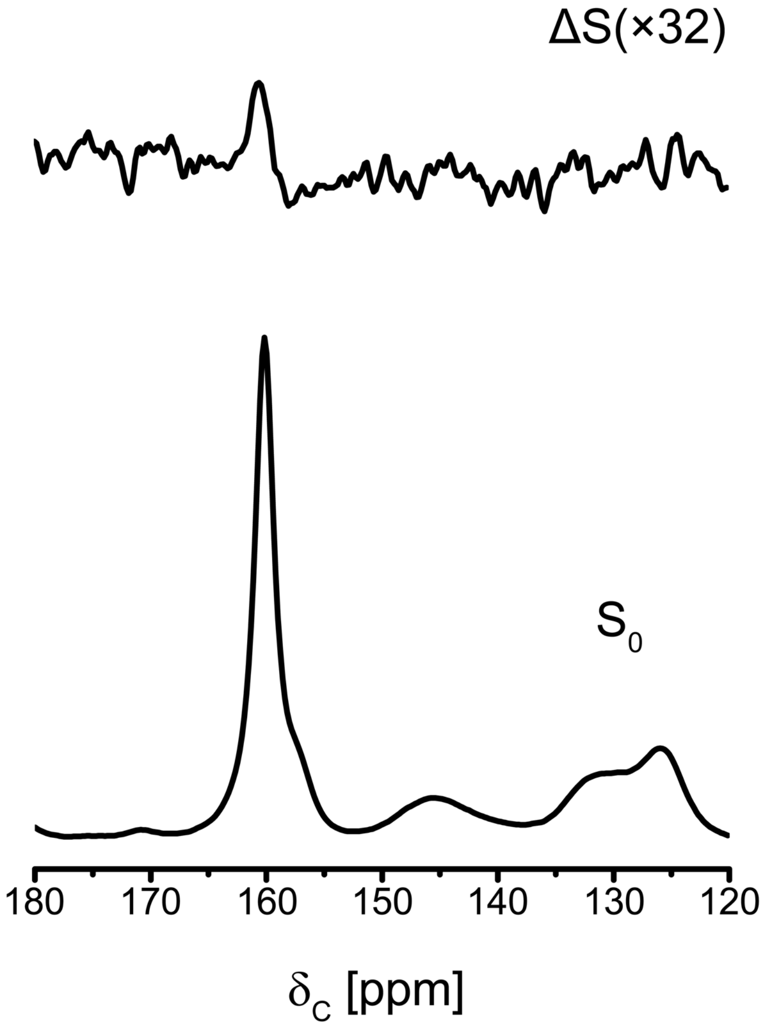

Figure S5. $^{13}C\{^{15}N\}$ REDOR spectra of the $^{13}CO_2$-absorbed sorbent after a 4.48 ms dephasing time.

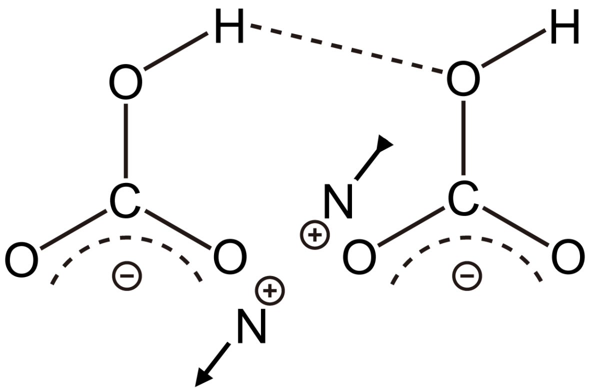

Figure S6. A possible structure of the absorbed HCO_3^-. The arrow indicates that ammonium cations are above and below the plane of the bicarbonate anions.

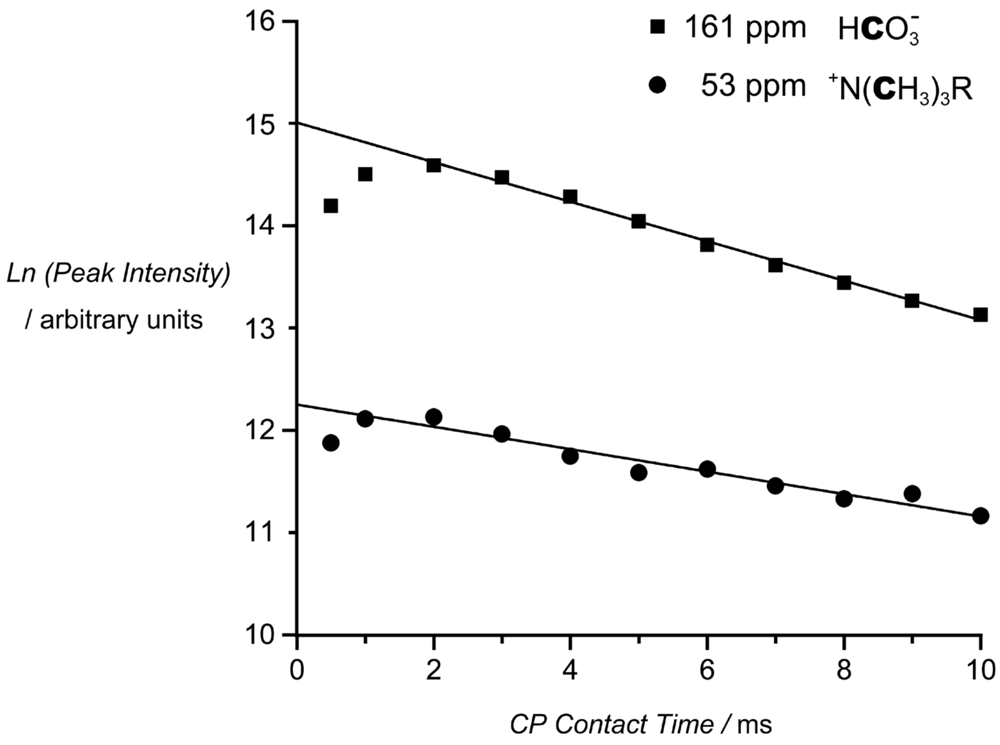

Figure S7. Carbon peak intensities from ^{13}C CPMAS spectra as a function of the length of the cross-polarization contact time for the $^{13}CO_2$-absorbed sorbent. Back-extrapolation to zero contact time provides relative intensities for both HCO_3^- carbon and $^+N(CH_3)_3R$ methyl carbons,[11] which here are $e^{15.00}$ and $e^{12.25}$, respectively. Because each binding site ($^+N(CH_3)_3R$) has three natural-abundance (1.11% ^{13}C) methyl carbons and the $^{13}CO_2$ is 90%-^{13}C enriched, we conclude that about 57% $\left(\frac{(\exp 15.00)\times\frac{1}{0.90}}{(\exp 12.25)\times\frac{1}{0.011}\times\frac{1}{3}}\right)$ of the binding sites are occupied.

Comparison of the amount of CO_2 cycled based on NMR observation and based on previous standard laboratory testing.

The CO_2 capture conditions in the standard laboratory testing of Matyjaszewski's group (He H *et al*., *Energy Environ. Sci.* 2013, 6, 488-493) are different from ours because we have different research purposes. In the work of Matyjaszewski's group, the goal was to test the feasibility of the humidity-swing CO_2 capture idea in a real environment. Thus they supplied CO_2 at a low concentration of 400 ppm to mimic the CO_2 concentration in the atmosphere. They also used a humidity cycle between 5 and 20 ppt (corresponding to 20 and 95% relative humidity) to mimic the likely humidity levels used in real applications. By contrast, our goal was to illuminate the chemical mechanism of the humidity-swing CO_2 capture/release cycle. Thus we supplied pure CO_2 gas (90% ^{13}C-enriched) instead of 400 ppm CO_2. We also lyophilized the sorbent to mimic dry conditions which is significantly dryer than 5 ppt (20% relative humidity) used by Matyjaszewski's group. Our goal was to maximize the absorbed CO_2 to enhance the NMR sensitivity to help identify the involved chemical species in the humidity-swing cycle.

The amount of CO_2 cycled in our experiments is higher than that of Matyjaszewski's experiments. This is consistent with the differences in the experimental conditions. We observed a CO_2 binding capacity of 30 to 57% (see main text and Figure S7), whereas Matyjaszewski's group observed a CO_2 binding capacity of 6 to 17% (Excellion membrane: 8%; Excellion active resin: 6%; carbon black templated sorbent: 6%; collodial crystal templated sorbent: 8%; HIPE templated sorbent: 17%). These CO_2 binding capacities in percentage were converted from the reported swing size in mmol/g (Table 1 of He H *et al*., *Energy Environ. Sci.* 2013, 6, 488-493).

References

(1) Morcombe, C. R.; Zilm, K. W. Chemical shift referencing in MAS solid state NMR. *J. Magn. Reson.* **2003,** *162* (2), 479-486.

(2) Stueber, D.; Mehta, A. K.; Chen, Z. Y.; Wooley, K. L.; Schaefer, J. Local order in polycarbonate glasses by $^{13}C\{^{19}F\}$ rotational-echo double-resonance NMR. *J. Polym. Sci., Part B: Polym. Phys.* **2006,** *44* (19), 2760-2775.

(3) Gullion, T.; Schaefer, J. Rotational-echo double-resonance NMR. *J. Magn. Reson.* **1989,** *81* (1), 196-200.

(4) Gullion, T.; Schaefer, J. Detection of weak heteronuclear dipolar coupling by rotational-echo double-resonance nuclear magnetic resonance. *Adv. Magn. Reson.* **1989,** *13*, 57-83.

(5) Mueller, K. T.; Jarvie, T. P.; Aurentz, D. J.; Roberts, B. W. The REDOR transform: direct calculation of internuclear couplings from dipolar-dephasing NMR data. *Chem. Phys. Lett.* **1995,** *242* (6), 535-542.

(6) Gullion, T.; Baker, D. B.; Conradi, M. S. New, compensated Carr-Purcell sequences. *J. Magn. Reson.* **1990,** *89* (3), 479-484.

(7) Gullion, T.; Schaefer, J. Elimination of resonance offset effects in rotational-echo, double-resonance NMR. *J. Magn. Reson.* **1991,** *92* (2), 439-442.

(8) Duncan, T. M. *Principal Components of Chemical Shift Tensors: A Compilation*; Farragut Press: Madison, United States, 1997; p. C-58.

(9) Levitt, M. H. *Spin Dynamics: Basics of Nuclear Magnetic Resonance*; 2nd ed.; John Wiley & Sons: Chichester, United Kingdom, 2008; p. 205.

(10) Bak, M.; Rasmussen, J. T.; Nielsen, N. C. SIMPSON: A general simulation program for solid-state NMR spectroscopy. *J. Magn. Reson.* **2000,** *147* (2), 296-330.

(11) McDowell, L. M.; Schmidt, A.; Cohen, E. R.; Studelska, D. R.; Schaefer, J. Structural constraints on the ternary complex of 5-enolpyruvylshikimate-3-phosphate synthase from rotational-echo double-resonance NMR. *J. Mol. Biol.* **1996,** *256* (1), 160-171.